Adsorption-desorption model and its application to vibrated granular materials

J. Talbot,[1] G. Tarjus,[2] and P. Viot[2,3]
[1]*Department of Chemistry and Biochemistry, Duquesne University, Pittsburgh, Pennsylvania 15282-1530*
[2]*Laboratoire de Physique Théorique des Liquides, Université Pierre et Marie Curie, 4 place Jussieu, 75252 Paris Cedex 05, France*
[3]*Laboratoire de Physique Théorique, Batîment 21, Université Paris–Sud, 91405 Orsay Cedex, France*
(Received 15 October 1999)

We investigate both analytically and by numerical simulation the kinetics of a microscopic model of hard rods adsorbing on a linear substrate, a model that is relevant for compaction of granular materials. The computer simulations use an event-driven algorithm that is particularly efficient at very long times. For a small, but finite desorption rate, the system reaches an equilibrium state very slowly, and the long-time kinetics display three successive regimes: an algebraic one where the density varies as $1/t$, a logarithmic one where the density varies as $1/\ln(t)$, followed by a terminal exponential approach. The characteristic relaxation time of the final regime, though incorrectly predicted by mean field arguments, can be obtained with a systematic gap-distribution approach. The density fluctuations at equilibrium are also investigated, and the associated time-dependent correlation function exhibits a power law regime followed by a final exponential decay. Finally, we show that denser particle packings can be obtained by varying the desorption rate during the process.

PACS number(s): 68.45.Da, 61.43.−j, 64.70.Pf

I. INTRODUCTION

The packing of granular materials is somewhat paradoxical. A child learns quickly that it is necessary to shake a bucket in order to pack the sand inside, but physicists cannot provide a completely satisfactory explanation of the densification process. The absence of a reference model, like the hard-sphere fluid for liquid-state physics or Ising model for phase transitions and magnetism, is at the origin of the slow progress in this field, despite a renewal of interest in recent years [1].

To capture the main features of the packing mechanism, the experimental study of a model system as simple as possible can help in building a reference theory. In this spirit, Knight *et al.* [2] have considered a system of monodisperse spherical beads. The packing process is realized by placing beads in a column that is tapped periodically with a given intensity. In a first series of experiments, they demonstrated that the density increases monotonically with the number of taps for various intensities of tapping. The very slow increase of density was analyzed, and a formula expressing the density in terms of the inverse of the logarithm of the number of taps was shown to be more accurate than any of the other suggestions [2]. Such behavior is common to models whose geometric exclusion effects dictate the kinetics of densification, i.e., models in which addition of new particles is exponentially limited by the inverse of the free volume [3–7].

In a second series of experiments, Nowak *et al.* [8,9] showed the presence of reversible/irreversible cycles. The beads in an initially loosely compacted state were vibrated for fixed periods with a sequence of increasing vibrational intensity, causing the density to increase monotonically. The sequence was then reversed so that the powder was vibrated with decreasing intensity. The density, however, continued to *increase* showing that the initial branch is irreversible. When the initial sequence of increasing vibration was repeated, the second branch was retraced confirming that it is reversible.

In the same experiments, Nowak *et al.* [8,9] monitored the power spectrum of the density fluctuations around the steady state for different values of the tapping strength. A two-step spectrum was observed characterized by two frequencies that both increase with increasing tapping strength. To account for the slow kinetics of compactification, the existence of a ''reversible'' steady state, and the fluctuation power spectrum, they proposed a simple adsorption-desorption or ''parking lot'' model.

The model describes the kinetics of densification of a given slice or layer of the material, perpendicular to the tapping force. (In the experiments, the tapping force is vertical, opposite to gravity.) Note that in the bulk region of the vibrated material, all slices are equivalent, as shown in Refs. [8] and [9]. As a result of a tapping event, particles leave the layer essentially at random. Densification proceeds when particles fall back into the layer under the influence of gravity, and the system reaches a new state of mechanical stability where particles are at rest. This is described in the model by a desorption/adsorption process, the ratio of desorption to adsorption rates being an increasing function of the tapping strength. Furthermore, no diffusion is allowed within a layer, which ensures that the particles are jammed in the absence of external forces. Of course, this approach accounts for the interlayer and mechanical stability effects only in an effective way. The physical situation corresponds to a two-dimensional layer. However, the same qualitative features are expected in the one- and two-dimensional versions of the model.

Partial analyses of this model have already been reported [10–12]. We present here a comprehensive description of the kinetics, including the final exponential regime and of the fluctuations around the steady state (equilibrium). We first present the model in Sec. II. We detail in Sec. III the specific algorithm that we have developed for enhancing the frequency of rare events in the late stages of the densification

process. In Sec. IV we study the densification kinetics. By using a gap distribution analysis we derive an expression for the time of relaxation towards equilibrium and the form of the gap distribution function in the limit of small desorption; the results compare very well with the simulation data. A short account of this derivation has been given in Ref. [13]. In Sec. V, the time-dependent density-density correlation function is studied in the equilibrium state. The correlation function displays two well-separated timescales, corresponding to two relaxation steps, and this can be interpreted by a simple model. In Sec. VI, we show that a faster densification can be obtained by changing the adsorption rate during the process.

II. MODEL

In the adsorption-desorption model, particles are placed in a D-dimensional space at randomly selected positions with a constant rate k_+. If the trial particle does not overlap any previously adsorbed particle, the new particle is accepted. In addition, all adsorbed particles are subject to removal (desorption) at random with a constant rate k_-. The one-dimensional version of the model, in which the substrate is a line and the objects are hard rods, has been solved in some limiting cases. When $k_-=0$, the adsorption is totally irreversible and the process corresponds to a one-dimensional (1D) random sequential adsorption (RSA) for which the kinetics are known exactly [14]. Without a relaxation mechanism, this process is driven towards a nonequilibrium state and the long-time kinetics are given by an algebraic scaling law, $\rho_\infty-\rho(t)\sim 1/t$, with $\rho_\infty\simeq 0.747\ldots$ (when the substrate is empty at the beginning of the process). When $k_+=0$, starting with any configuration of particles, one obtains an analytical solution for this uniform desorption process [15]. The limit $k_-\to 0^+$, which allows a small but nonzero possibility of rearrangement of the particles on the line, leads to a final density equal to 1. It is worth noting the finite discontinuity between the final density of this case ($k_-\to 0^+$) and the RSA jamming limit ($k_-=0$). Moreover, the final density is independent of the initial configuration of particles on the line, whereas the jamming limit for the RSA process depends strongly on the initial state of the line. For $k_-\to 0^+$, accurate descriptions have been obtained [10,11]. In this case, the process cleanly divides into two sub-processes. The initial phase consists of an irreversible adsorption and it is followed by an infinite sequence of desorption-adsorption events in which a rod detaches from the surface and the gap that is created is immediately filled by one or two new rods. The latter possibility causes the system to evolve continuously to the close-packed state with $\rho=1$ as [10,11] $1-\rho(t)\simeq 1/\ln(t)$ where t now represents a rescaled time. For the general case, where both k_+ and k_- are nonzero, a complete solution is not available.

The properties of the adsorption-desorption model depend only on the ratio $K=k_+/k_-$. A large value of K then corresponds to a small desorption rate. If time is expressed in units of k_+^{-1}, the densification kinetics is given by

$$\frac{d\rho}{dt}=\Phi(t)-\frac{\rho}{K}, \tag{1}$$

where $\Phi(t)$, the insertion probability, is the fraction of the substrate that is available for the insertion of a new particle. The presence of a relaxation mechanism, i.e., competing desorption and adsorption with an equilibrium constant K, implies that the system eventually reaches a steady state that corresponds to an equilibrium configuration of hard particles with $\rho_{\rm eq}=K\Phi_{\rm eq}(\rho_{\rm eq})$, where $\rho_{\rm eq}$ denotes the equilibrium density. At equilibrium, the insertion probability is given exactly by

$$\Phi_{\rm eq}(\rho)=(1-\rho)\exp[-\rho/(1-\rho)]. \tag{2}$$

Inserting Eq. (2) in Eq. (1) leads to the following expression for the equilibrium density:

$$\rho_{\rm eq}=\frac{L_w(K)}{1+L_w(K)}, \tag{3}$$

where $L_w(x)$ (the Lambert-W function) is the solution of $x=ye^y$. In the limit of small K, the isotherm takes the Langmuir form, $\rho_{eq}\sim K/(1+K)$, while for large K, $\rho_{eq}\sim 1-1/\ln(K)$. At small values of K, equilibrium is rapidly obtained, but at large values the densification process is dramatically slowed.

III. SIMULATION ALGORITHM

A naive method of simulating the adsorption-desorption process would attempt to randomly insert a new particle at fixed time intervals. This approach, however, is extremely inefficient at high densities since most attempts to add new particles are unsuccessful after an initial period. We have developed a general algorithm that enables us to investigate in detail the kinetics of the adsorption process at arbitrarily long times and for arbitrarily large values of the equilibrium constant K. Instead of using a fixed time step, the algorithm is based on adsorption or desorption *events*. In this section we describe the general features of the algorithm that could be to simulate an adsorption-desorption process of arbitrarily shaped particles in any dimension. Later, we detail the methodology for the hard-rod system.

The total rate of adsorption and desorption events is

$$R_{\rm tot}(t)=\Phi(t)+\rho(t)/K. \tag{4}$$

The quiesence, or waiting time, is the time interval between any two successive events that alter the state of the system. Let $F(\tau)$ denote the probability that the waiting time is greater than τ. Since successive events are considered to be independent,

$$F(\tau+\Delta\tau)=F(\tau)[1-R_{\rm tot}\Delta\tau+O(\Delta\tau^2)]. \tag{5}$$

Taking the limit $\Delta\tau\to 0$ we obtain

$$F(\tau)=\exp(-R_{\rm tot}\tau). \tag{6}$$

A uniformly distributed random number, $0<\xi_1<1$, may be used to sample a random waiting time consistent with this distribution:

$$\tau=-\ln(\xi_1)/R_{\rm tot}. \tag{7}$$

Once the quiesence time has been selected, the nature of the event is determined stochastically by defining

$$r_d(t)=\frac{\rho(t)/K}{R_{\rm tot}(t)} \tag{8}$$

and choosing a second uniformly distributed random number, $0<\xi_2<1$. If $\xi_2<r_d(t)$ the event at time t is a desorption and a randomly selected particle is removed from the system. If $\xi_2>r_d(t)$ the event is an adsorption and a new particle is placed randomly in the available surface. We have validated the method by applying it to the Langmuir equation where $\Phi=1-\rho/\rho_{max}$ and the kinetics, as well as the isotherm, are known exactly. This method is quite general and can apply to a range of adsorption-desorption processes.

In the simulation, the initial state of the system is an interval of length L (measured in rod lengths) bounded by two immovable rods centered at positions $x_0=-1$, $x_{N+1}=L+1$. For an arbitrary configuration of N additional rods, whose centers are located at $\{x_i, i=1,\ldots,N\}$, the total available length is known exactly: $L_0=\sum_{i=0}^{N+1}\max(x_{i+1}-x_i-2,0)$. At each step of the simulation, the total rate of adsorption and desorption events is determined from $R=L_0+N/K$. A waiting time is sampled from the exponential waiting time distribution using Eq. (7) and the type of event is decided with Eq. (8). If the event is adsorption, a new particle is placed in the available length. The probability that a particular gap is occupied is equal to its available length divided by the total available length L_0. Thus, a random number ξ_3 is generated and the position of the particle on the available length is $\xi_3 L_0$, which means that the gap between particles j and $j+1$ is occupied where j is defined by the following equation

$$\sum_{i=0}^{j-1}\max(x_{i+1}-x_i-2,0)<\xi_3 L_0<\sum_{i=0}^{j}\max(x_{i+1}-x_i-2,0). \tag{9}$$

Note that the adsorption event is uniform and is always accepted. If the event is desorption a particle is selected at random and removed from the surface. Note that the desorption probability is independent of the length of time that the particle has been on the surface. The available line is updated; it always decreases (increases) following an adsorption (desorption) event. The simulation procedure thus generates a sequence of configurations $(t_1,N_1,L_{01}),(t_2,N_2,L_{02}),\ldots$ and one knows the state of the system at an arbitrary time, t. To insure good statistics, several thousands of independent simulations must be run for each value of the desorption rate. We used system lengths, L, from 400 to 5000.

IV. GAP DENSITY APPROACH

The adsorption-desorption model can be described in terms of gap distribution functions. The one-gap distribution function, $G(h,t)$, represents the density of voids of length h; the time evolution of $G(h,t)$ is given by

$$\frac{\partial G(h,t)}{\partial t}=-H(h-1)(h-1)G(h,t)+2\int_{h+1}^{\infty}dh'\,G(h',t)-\frac{2}{K}G(h,t)+\frac{H(h-1)}{K\rho(t)}\int_0^{h-1}dh'\,G(h',h-1-h',t), \tag{10}$$

where $G(h,h',t)$ is the two-gap distribution function associated with the probability of finding two *neighboring* gaps (separated by one particle) of length h and h', and $H(x)$ is the Heaviside step function [$H(x)=1$ for $x>1$, $H(x)=0$ otherwise]. The first two terms on the right-hand side of Eq. (10) correspond to loss and gain terms due to adsorption while the remaining two are due to desorption. Similarly, the time evolution of $G(h,h',t)$ is given by

$$\begin{aligned}\frac{\partial G(h,h',t)}{\partial t}=&-[H(h-1)(h-1)+H(h'-1)(h'-1)]G(h,h',t)\\&+\int_{h+1}^{\infty}dh''G(h'',h',t)+\int_{h'+1}^{\infty}dh''G(h,h'',t)\\&+G(h+h'+1,t)-\frac{3}{K}G(h,h',t)\\&+\frac{H(h-1)}{K\rho(t)}\int_0^{h-1}dh''G(h'',h-1-h'',h',t)\\&+\frac{H(h'-1)}{K\rho(t)}\int_0^{h'-1}dh''G(h,h'-1-h'',h'',t),\end{aligned} \tag{11}$$

where $G(h,h',h'',t)$ is the three-gap distribution function. The kinetics of the process is thus given by an infinite hierarchy of equations involving an infinite set of multi-gap distribution functions.

The quantities of interest can be expressed in terms of integrals of the one-gap distribution function. In particular, the insertion probability $\Phi(t)$ is given by

$$\Phi(t)=\int_1^{\infty}dh(h-1)G(h,t), \tag{12}$$

and we have the following sum rules:

$$\rho(t)=\int_0^{\infty}dh\,G(h,t), \tag{13}$$

and

$$1-\rho(t)=\int_0^{\infty}dh\,h\,G(h,t). \tag{14}$$

[One also has $\rho(t)G(h,t)=\int_0^{\infty}dh'\,G(h,h',t)=\int_0^{\infty}dh'\,G(h',h,t)$ and similar integrals for higher-order

terms.] The steady-state solution of Eq. (10) is known and corresponds to the equilibrium hard-rod system with a gap distribution function given by [10,11]

$$G_{\mathrm{eq}}(h,\rho)=\frac{\rho^2}{1-\rho}\exp\left(-\frac{\rho}{1-\rho}h\right), \tag{15}$$

and all higher-order distribution functions satisfying the factorization property,

$$G_{\mathrm{eq}}(h_1,h_2,\ldots,h_n,\rho) = G_{\mathrm{eq}}(h_1,\rho)G_{\mathrm{eq}}(h_2,\rho)\cdots G_{\mathrm{eq}}(h_n,\rho). \tag{16}$$

In order to find a solution for the kinetics of the process, one must truncate the hierarchy by means of a closure ansatz. The simplest closure is provided by an adiabatic (mean-field) treatment. There, one assumes that, at any density $\rho(t)$, the structure of the adsorbate, as characterized by the gap distribution functions, is that of an equilibrium system at density $\rho(t)$.

V. DENSIFICATION KINETICS (AT CONSTANT $K\gg 1$)

A. A succession of regimes

We focus here on the small desorption limit ($K\gg 1$). For an initially empty line, there are three different successive kinetic regimes. The first stage is dominated by adsorption events and the process displays an RSA-like behavior, characterized by a $1/t$ power law dependence. For $\rho(t)\geqslant 0.7$, adsorption becomes slower and desorption can no longer be ignored, which allows particle rearrangements on the line and, eventually, insertion of additional particles. The densification mechanism requires the rearrangement of an increasing number of particles in order to open a hole large enough for the insertion of an additional particle. The process is similar to what occurs in the limit $k\to 0^+$, and the kinetics is dominated by a $1/\ln(t)$ behavior [10,11]. For large but finite values of K, this densification regime continues until the density is very close to the equilibrium (steady-state) value, $\rho_{\mathrm{eq}}(K)$. In the final regime, the desorption term becomes comparable to the adsorption term, and an exponential approach to equilibrium is observed. Figure 1 illustrates the three successive regimes.

B. Exponential approach to equilibrium

The exponential regime is illustrated in Fig. 2(a). In an adiabatic (mean-field) treatment the insertion probability, $\Phi(t)$, satisfies an equation similar to Eq. (2) with $\rho(t)$ in place of ρ_{eq}. Denoting $\delta\rho(t)=\rho(t)-\rho_\infty$, with $\rho_\infty=\rho_{eq}(K)$, one obtains from Eq. (1), at first order in density,

$$\frac{d}{dt}\delta\rho=-\Gamma_{MF}(K)\,\delta\rho+O(\delta\rho^2) \tag{17}$$

with

$$\Gamma_{MF}(K)=\frac{[1+L_w(K)]^2}{K}, \tag{18}$$

$$\simeq \ln(K)^2/K \quad \text{when K is large}, \tag{19}$$

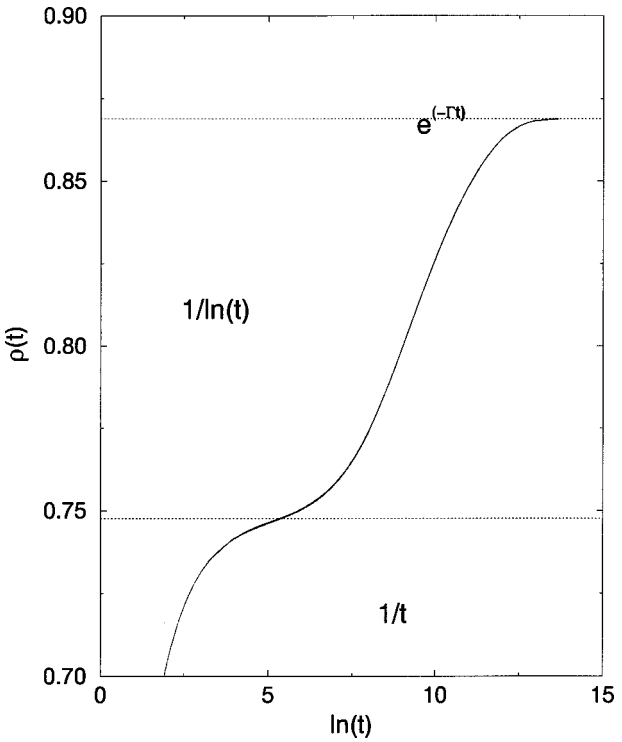

FIG. 1. Linear-logarithmic plot of the adsorbed density as a function of time for a large value of K ($K=5000$). The process is characterized by three slow kinetic regimes: (i) RSA-like regime whose final stage is described by a $1/t$ behavior, (ii) $1/\ln(t)$ regime, and (iii) exponential approach towards equilibrium.

which is equivalent to a relaxation time given by $K/\ln(K)^2$ for large K.

In Fig. 2(b), the relaxation rate is plotted as a function of K: the dashed curve gives the mean-field prediction, Eq. (19), and open circles correspond to the best exponential fit to the simulation results. It is evident that the mean-field analysis gives a poor estimate of the relaxation rate for large K. This failure can be understood by noting that the mean-field assumption leads to a characteristic time for the rearrangement of Φ of the order $K/\ln(K)^2$, i.e., much smaller than K, the characteristic time for desorption. Since in the absence of surface diffusion process, significant rearrangement can only occur on a timescale longer than K the system is unable to adjust rapidly enough in order to change significantly the available surface function on a timescale of order $K/\ln(K)^2$. In Fig. 3, we display the insertion probability, $\Phi(\rho)$, for several large values of K; it is worth noting that Φ first follows the RSA curve until it reaches a value close to the equilibrium one at which point it plateaus and evolves very weakly towards equilibrium. The process clearly deviates from the adiabatic description in which the insertion probably is given, at all densities, by the equilibrium curve, $\Phi_{\mathrm{eq}}(\rho)$.

We now turn to a description in terms of the gap distribution approach. To obtain the leading term in the exponential approach towards equilibrium, when K is very large (but finite), we assume that, as for the steady state (or equilibrium), $|G(h,t)|\sim\exp(-\Pi h)$, with $\Pi\sim\ln K\sim(1-\rho)^{-1}$ [see Eqs. (15) and (3), when K is very large]. As a consequence, if one defines $\rho_n(t)=\int_n^{n+1}G(h,t)dh$ and $\Phi_n(t)=\int_n^{n+1}(h-1)G(h,t)dh$, then $\rho_n\sim\Phi_n\sim K^{-n}$, so that if one looks for

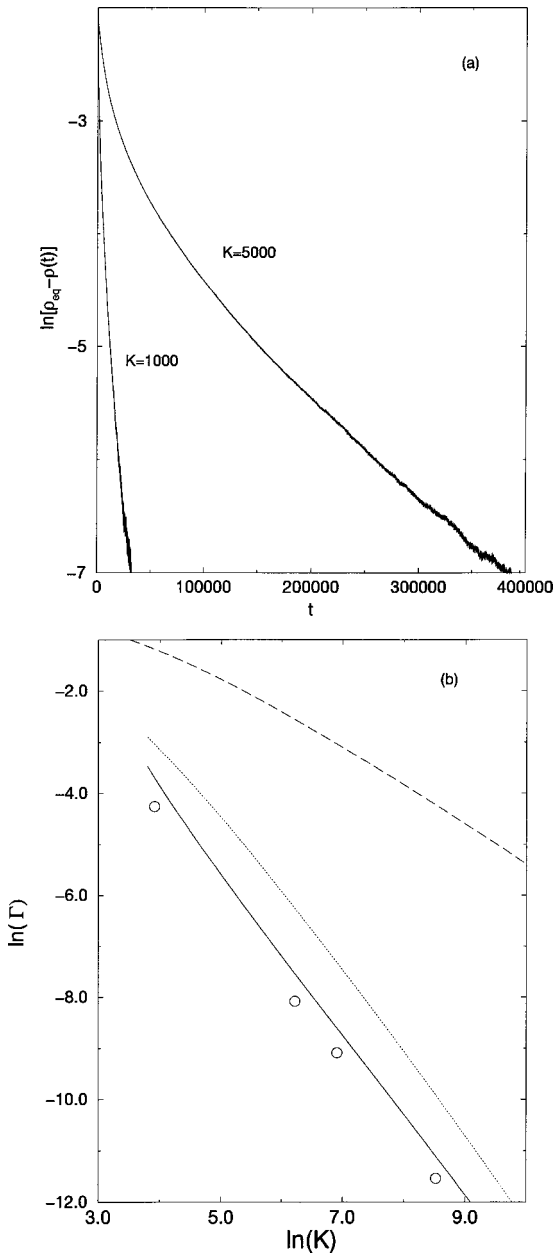

FIG. 2. (a) Final exponential approach of the density ρ to its equilibrium value ρ_{eq} for two large values of K. (b) Relaxation rate for the approach to equilibrium Γ versus K. Upper curve: prediction from mean-field approximation, Eq. (19). Dotted curve: leading term of Eq. (32). Full curve, Eq. (A17) . Open circles: best exponential fit to the numerical simulations.

the dominant behavior in $1/K$, it is sufficient to consider the first intervals in h. As in the adiabatic approximation, one can expand the gap densities in power of $\delta\rho(t)$ and keep only the linear term which gives rise to the exponential decay. In the final regime, where the density is close to the steady state, we first assume that the deviation of the gap distribution function from its equilibrium form, $\delta G(h,t) = G(h,t) - G_{eq}(h)$, can be expressed as an expansion in $\delta\rho(t)$ where only the first term is kept. Let us then denote

$$A(h) = \rho_\infty \left. \frac{\partial \ln G(h,\rho)}{\partial \rho} \right|_{\rho_\infty} \tag{20}$$

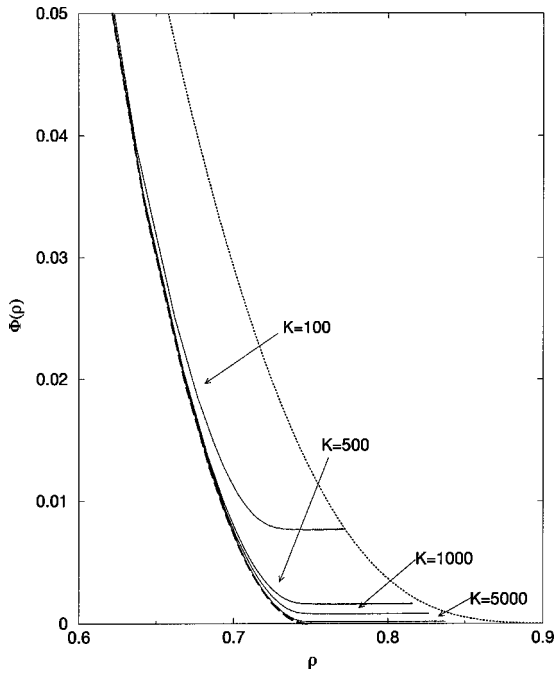

FIG. 3. The insertion probability Φ as a function of density ρ for various large values of K ($K=100,500,1000,5000$). The dashed curve corresponds to a process without desorption (RSA process) and the dotted curve corresponds to the equilibrium insertion probability, Eq. (2).

and

$$A(h,h') = \rho_\infty \left. \frac{\partial \ln G(h,h',\rho)}{\partial \rho} \right|_{\rho_\infty}. \tag{21}$$

After inserting Eq. (20) in Eq. (10) $A(h)$ can be rewritten for $0<h\leqslant 1$ as

$$\frac{2-\gamma}{K} A(h) = \frac{2P_\infty}{K} \int_h^{+\infty} dh' e^{-P_\infty(h'-h)} A(1+h'), \tag{22}$$

where $P_\infty = \rho_\infty/(1-\rho_\infty)$ is the dimensionless equilibrium pressure for $\rho_\infty = \rho_{eq}$ and

$$\gamma = K\Gamma = -K \frac{d}{dt} \delta\rho(t)/\delta\rho(t)|_{\rho_\infty}. \tag{23}$$

From Eqs. (1) and (12), one obtains

$$\gamma = 1 - P_\infty^2 \int_0^\infty dh h e^{-P_\infty h} A(1+h) \tag{24}$$

whereas the sum rules in Eqs. (13) and (14) give, respectively,

$$P_\infty \int_0^\infty dh e^{-P_\infty h} A(h) = 1 \tag{25}$$

$$-P_\infty \int_0^\infty dh h e^{-P_\infty h} A(h) = 1. \tag{26}$$

When integrating the two sides of Eqs. (22) between 0 and 1, one obtains

$$(2-\gamma)=2P_\infty^2\int_0^1 dhhe^{-P_\infty h}A(1+h)+O(1/K). \quad (27)$$

Combining Eq. (24) with Eq. (27) yields $\gamma=O(1/K)$. Thus, the relaxation rate Γ goes essentially as $1/K^2$ instead of the $1/K$ dominant behavior predicted by the mean-field treatment. In order to have a more explicit expression for γ and Γ, it is necessary to calculate the integral on the right-hand side of Eq. (24) to $O(1/K^2)$

$$(2-\gamma)\left\{1-\frac{P_\infty^2}{K}\left[\int_0^1 e^{-P_\infty h}A(1+h)+A(1)\right]\right\}$$
$$=2-2\left[\gamma-\frac{P_\infty^3}{K}\int_0^1(h+1)e^{-P_\infty h}A(2+h)\right]+O(1/K^2), \quad (28)$$

which leads to

$$\gamma K=2P_\infty\left[A(0)+P_\infty A(1)-P_\infty^2\int_0^1(h+1)e^{-P_\infty h}A(2+h)\right]+O(1/K). \quad (29)$$

An explicit expression for γK, Eq. (29) thus requires the knowledge of the gap distribution function for $3>h>1$. The kinetic equation for the gap distribution function when $h>1$ is then rewritten by inserting Eqs. (20) and (21) in Eq. (10), which gives

$$\left(h-1+\frac{2-\gamma}{K}\right)A(h)=-(h-1)+\int_0^{h-1}dh'A(h',h-1-h')+\frac{2P_\infty}{K}\int_{h-1}^{\infty}dhe^{-P_\infty(h'-h)}A(1+h). \quad (30)$$

Combining Eq. (29) and Eq. (30) for $h=1$, one finally gets

$$\gamma K=2P_\infty\left[A(0)-P_\infty^2\int_0^1 dhhe^{-P_\infty h}A(2+h)\right]+O(1/K). \quad (31)$$

Since the system evolves close to equilibrium, we further assume that the factorization property for the two-gap distribution function is valid to $O(1/K)$, i.e., $A(h,h')=A(h)+A(h')+O(1/K)$ [16]. Equations (30) and (22) then become a closed set of equations for $A(h)$ to $O(1/K)$. The solution is given in the Appendix, as well as the explicit expression for $\Gamma(K)=\gamma/K$, Eq. (A17). As an illustration, the leading terms of $\Gamma(K)$ in powers of $\ln(K)$ are obtained as

$$\Gamma\simeq 2\frac{(\ln K)^3}{K^2}-4\frac{(\ln K)^2}{K^2}+2\frac{(\ln K)}{K^2}+O\left(\frac{1}{K^2}\right). \quad (32)$$

The prediction of Eq. (A17), shown as the full curve in Fig. 2(b), gives a good agreement with the results obtained from an exponential fit to the simulation data, whereas the mean-field prediction fails completely (dashed curve) [the dotted curve corresponds to the first term of the right hand-side of Eq. (32)].

VI. FLUCTUATIONS AROUND EQUILIBRIUM

For times much larger than the relaxation time, the density no longer evolves (on average), but fluctuates around its equilibrium value. Note that in this regime, the fluctuation-dissipation theorem and the time translational invariance are both valid. We have calculated the time-dependent correlation function $C(t)$ of the density fluctuations, $\delta\rho(t)=\rho(t)-\rho_\infty$, around the equilibrium state. Starting from the $2-$ time correlation function,

$$C(t'+t,t')=\frac{\langle\rho(t'+t)\rho(t')\rangle-\langle\rho(t'+t)\rangle\langle\rho(t')\rangle}{\langle\rho(t')^2\rangle-\langle\rho(t')\rangle^2}, \quad (33)$$

we have numerically verified that when $t'\gg 1/\Gamma$, $C(t'+t,t')$ becomes time translationnally invariant, i.e., $C(t'+t,t')=C(t)$. (Conversely, when $1\ll t'\ll 1/\Gamma$, one observes aging phenomena [17], but we postpone the discussion of this phenomena to a future publication.) Because of the very long relaxation time, we found that the calculation of the correlation function is more efficient by using Eq. (33) instead of taking the usual time average on a single system [18]. Results from the simulation are shown in Fig. 4 for two large values of K. At short and intermediate times, the decay of $C(t)$ is nonexponential, whereas at long times the kinetics follows an exponential decay. The two regimes, or relaxation steps, can be interpreted as follows: the first consists of a ''fast'' adsorption-desorption process without appreciable densification of the system, whereas the second corresponds to the linear-response regime and, as predicted by Onsager's regression hypothesis, it shows the same final exponential dependence as the final approach of $\rho(t)$ towards ρ_∞ in the densification process. In this second relaxation step, $C(t)\sim e^{-\Gamma t}$ where Γ is given by Eqs. (32) and (A17).

Close to equilibrium and for large values of K, the adsorption and desorption events can be considered as spatially uncorrelated, and the system can be represented as a set of independent gaps in which a particle is adsorbed or not. This assumption does not account for rearrangements that occur at long times, but is valid for short times. When a particle is adsorbed, the gap is characterized by the distribution $g_{eq}(h)$, which is the distribution probability of finding a particle such the total length of right and left gap is equal to h, i.e.,

$$g_{eq}(h)=\frac{1}{\rho_\infty}\int_0^h dh'G_{eq}(h')G_{eq}(h-h')$$
$$=\rho_\infty P_\infty^2 h\exp(-P_\infty h). \quad (34)$$

Once the particle has desorbed, the gap is characterized by the distribution $G_{eq}(h+1)$. The two distributions are calculated at equilibrium and their ratio is given exactly by:

$$\frac{G_{eq}(h+1)}{g_{eq}(h)}=\frac{1}{Kh}. \quad (35)$$

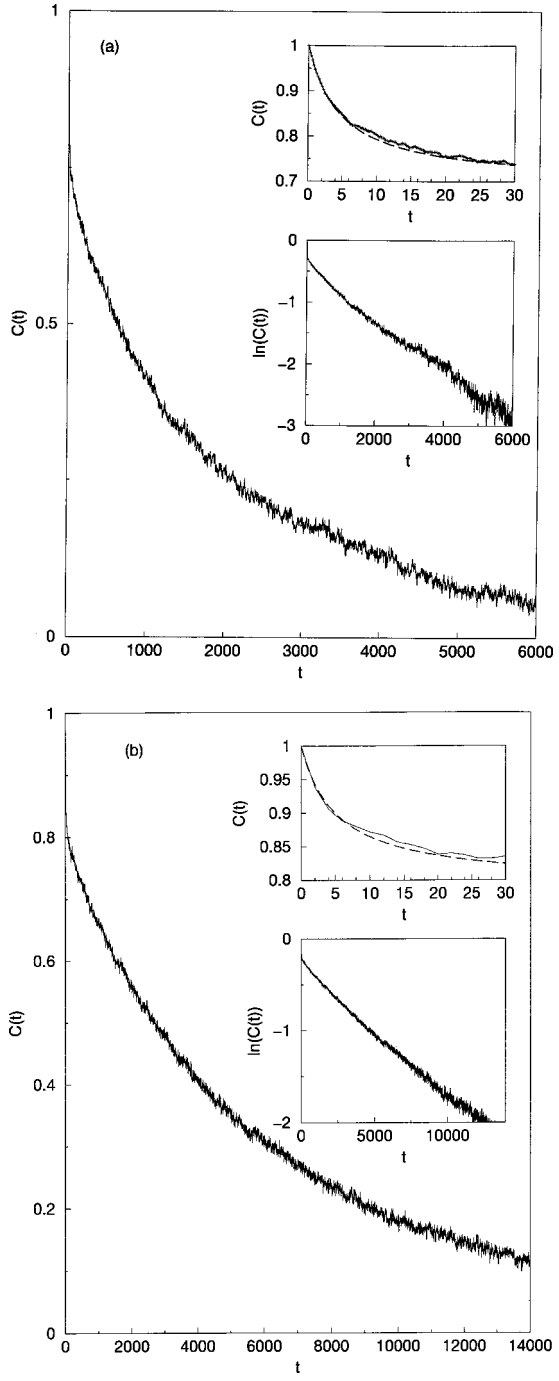

FIG. 4. Equilibrium density-density correlation function $C(t)$ versus time for (a) $K=500$ and (b) $K=1000$. The inset in the upper right corner displays the first step in the decay of the correlation function (full curve) as well as the predicted short-time formula, $C_{short}(t)$, Eq. (41) (dashed curve). The other inset shows the exponential decay of $C(t)$ at long times on a logarithmic-linear plot.

For a given gap of length $(h+1)$, we have a two-state (particle-hole) stochastic process in which the rates, associated to desorption and adsorption, respectively, are $1/K$ and h. The average probability for having a particle in the gap is equal to

$$P(h)=\frac{hK}{1+hK}. \tag{36}$$

For a given gap of length $(h+1)$, the (unnormalized) correlation function of the density fluctuations $\tilde{C}_h(t)$ due to the two-state stochastic process is given by [20]

$$\tilde{C}_h(t)=\frac{P(h)}{(1+hK)}\exp[-(1/K+h)t]. \tag{37}$$

Assuming that the adsorption-desorption events giving rise to the two-state process only seldom affect simultaneously two neighboring particles, one can write the (unnormalized) correlation function as a superposition of correlation functions occurring in parallel in the different gaps, weighted by the distribution $g_{eq}(h)$, i.e.,

$$\tilde{C}_{short}=\int_0^\infty dh g_{eq}(h)\tilde{C}_h(t) \tag{38}$$

$$\simeq\frac{\rho_\infty P_\infty^2}{K}\frac{\exp(-t/K)}{(t+P_\infty)}\,. \tag{39}$$

At equilibrium, the variance of the density fluctuations can be calculated exactly [21],

$$\langle(\delta\rho)^2\rangle=\rho_\infty(1-\rho_\infty)^2, \tag{40}$$

so that, the normalized correlation function $C(t)$ at short times, C_{short}, can be written as

$$C_{short}(t)\simeq\frac{P_\infty^2}{K(1-\rho_\infty)^2}\frac{\exp(-t/K)}{(t+P_\infty)}\,, \tag{41}$$

which reduces to a power law, $1/t$, when $\ln(K)\ll t\ll K$. This result is equivalent to the $\ln(\omega)$-behavior already predicted along similar lines similar by Kolan *et al.* [19]. The insets in Figs. 4(a) and 4(b) illustrate the excellent agreement between Eq. (39) and the simulation data.

It is worth noting that the $1/t$ behavior is reminiscent of the pure RSA asymptotic regime, where it occurs as a consequence of the filling of small isolated pieces of the available fraction of the line, whose lengths go to zero when $t\to\infty$. With similar arguments, one thus expects to have in higher dimensions a $t^{-1/D}$ behavior, leading to an $\omega^{(1-1/D)}$ power-law dependence for the power spectrum. In particular, this predicts a power law $\omega^{-1/2}$ for $D=2$, which is compatible with the experimental data in vibrated granular media [9]. In dimensions higher than 1, our prediction differs from that of Kolan *et al.* [19] since their analysis leads to a $1/\omega$ dependence in the power spectrum. A numerical study of the two-dimensional version of the adsorption-desorption model should settle this point.

VII. DENSIFICATION REGIME AND MULTISTEP PROCESS

The very slow-exponential approach to equilibrium with $\Gamma(K)=O(1/K^2)$ when K is very large implies that $\Phi(\rho)$ increases with ρ when ρ is sufficiently large (see Sec. V B and the Appendix). Since in the first (RSA-like) regime $\Phi(\rho)$ decreases, there always exists a density ρ_m where $\partial\Phi(\rho)/\partial\rho|_{\rho_m}=0$. Figure 5 displays a log-log plot of Φ as a function of time for various values of K. One notices (i) that

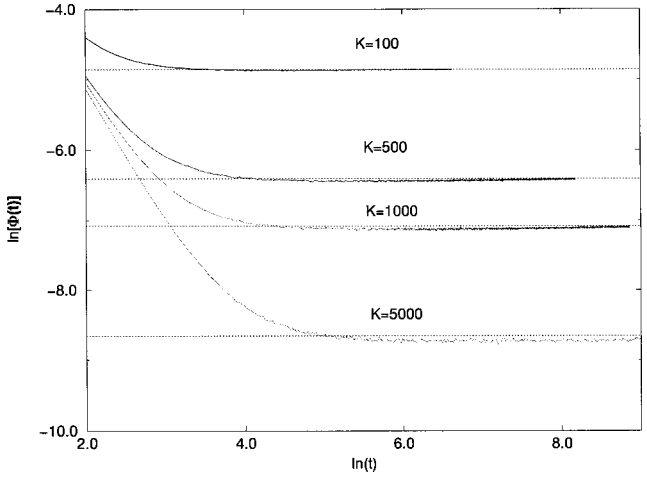

FIG. 5. Log-log plot of the insertion probability Φ as a function of time for various large values of K ($K=100,500,1000,5000$). Note that for $K>100$, Φ displays a minimum that is smaller than the equilibrium value (dotted lines).

ρ_m is an increasing function of K and (ii) that the minimum of Φ is always very close but smaller than the equilibrium value, $\Phi_{eq}(K)$, and smaller than ρ/K, which is due to the fact that the density is an increasing function of time.

In Fig. 6, the density is plotted as a function of time for different values of K. The curves on the left part of the figure correspond to an adiabatic process where the available surface function is replaced by the equilibrium formula, Eq. (2), and which corresponds to a process where rapid diffusion on the substrate allows an instantaneous equilibration after each desorption and adsorption event. For all values of K, the adiabatic process is much faster than the corresponding adsorption-desorption model process. Moreover, for an adiabatic process, the density is at all times always a monotonically increasing function of K. For the adsorption-desorption model, on the other hand, the density is *not always monotonic* in K. In Fig. 6, for example, the system with $K=500$ has a higher density than the system with $K=1000$ for $4 \lesssim \ln(t) \lesssim 8$. The existence of a minimum in Φ is a sufficient condition for this phenomenon. It follows that *for a given finite time*, the densification can be made more efficient by changing the desorption rate during the process. Figure 7 compares the densities obtained by using either a single value of $K=1000$ or a sequence of varying K, starting from 1000 at $t=0$, passing through a minimum, and finishing at the same value $K=1000$ when $t=1000$. One clearly observes that a larger final density is reached with the multistep process. Such a phenomenon, which is also the source of the reversible-irreversible cycles observed by Nowak *et al.* [9], has been already observed and quantitatively analyzed in an irreversible adsorption model [15]. However, the determination of the optimum densification strategy, which has significant applications to vibratory compaction of granular materials, is still an open problem.

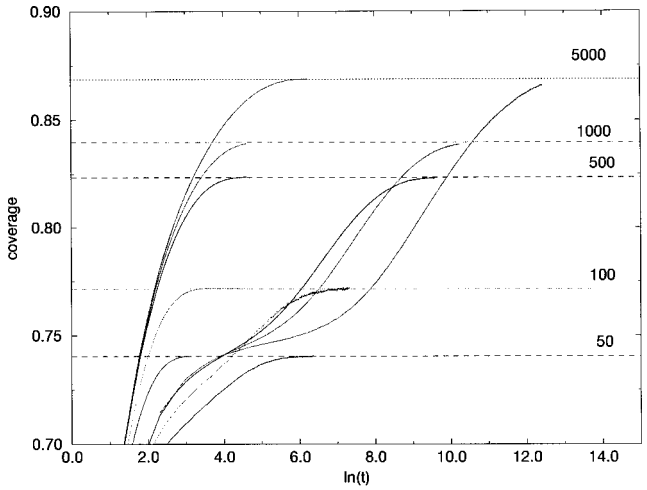

FIG. 6. Linear-log plot of the density versus time for different values of K. The left curves correspond to the adiabatic process. The right curves correspond to the adsorption-desorption model. Notice that in the latter case the curves for different values of K always cross, a phenomenon absent in the adiabatic process.

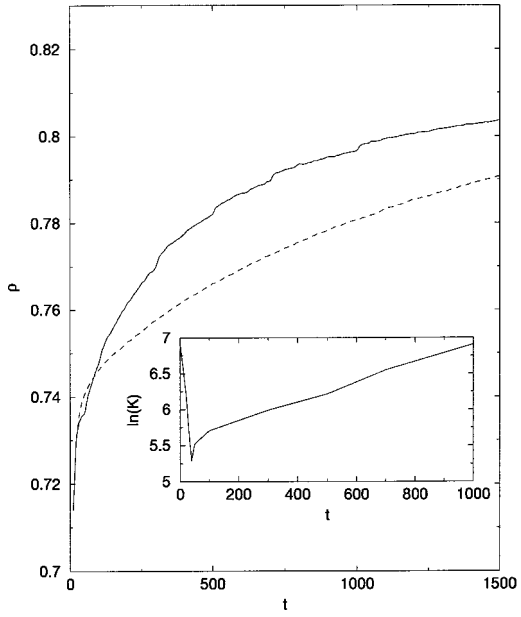

FIG. 7. Density increase over 1500 time units for a process with a single value of K ($K=1000$) and for multistep process in which the sequence of K is shown on a linear-logarithmic plot in the inset (after $t=1000$, K stays constant). Note the large enhancement of packing efficiency in the latter process. This effect is absent in the adiabatic approximation where the density is a monotonically increasing function of K.

ACKNOWLEDGMENTS

J.T. thanks the National Science Foundation for financial support. The Laboratoire de Physique Théorique des Liquides is Unité Mixte de Recherche No. 7600 au CNRS. The Laboratoire de Physique Théorique is Unité Mixte de Recherche No. 8627 au CNRS.

APPENDIX: SOLUTION FOR THE GAP DISTRIBUTION FUNCTION IN THE LINEAR RESPONSE REGION

For convenience, we introduce the notation $B(h)=A(h)-1$, $B(h,h')=A(h,h')-2$, etc. For $0 \leqslant h \leqslant 1$, by taking into account that $\gamma=O(1/K)$, Eq. (22) can be reexpressed as

$$B(h)e^{-P_\infty h}-B(1)\frac{P_\infty}{K}=P_\infty\int_0^1 dh' e^{-P_\infty h'}B(1+h') + O(e^{-P_\infty h}/K), \quad \text{(A1)}$$

and for larger gaps, Eq. (30) can be rewritten for $h\geqslant 0$, as

$$\left(h+\frac{2}{K}\right)B(1+h)=\int_0^h dh' B(h',h-h') + \frac{2P_\infty}{K}e^{P_\infty h}\int_h^\infty U_\infty dh' e^{-P_\infty h'}B(2+h') + O(1/K^2). \quad \text{(A2)}$$

Assuming that the factorization property is valid to a $O(1/K)$, i.e.,

$$B(h,h')=B(h)+B(h')+\frac{C(h,h')}{K}+O(1/K^2), \quad \text{(A3)}$$

with $0\leqslant h\leqslant 1$, and $O(1/K)$ or $O(1/K^2)$ designate functions that are uniformly of order $1/K$ or $1/K^2$ on the interval $[0,1]$, we can derive from Eq. (A2)

$$\left(h+\frac{2}{K}\right)B(1+h)-2\int_0^{h-1}dh' B(h') = \frac{1}{K}\left[\int_0^h dh' C(h',h-h') + 2P_\infty\int_h^\infty dh' e^{-P_\infty(h'-h)}B(2+h')\right]+O(1/K^2), \quad \text{(A4)}$$

and

$$(1+h)B(2+h)-2\int_0^{1+h}dh' B(h')=O(1/K). \quad \text{(A5)}$$

When $h\gg 2/K$, Eq. (A4) simplifies to

$$hB(1+h)-2\int_0^1 dh' B(h')=O(1/K). \quad \text{(A6)}$$

Deriving Eq. (A6) with respect to h and inserting the result in Eq. (A1), one gets the following differential equation,

$$\frac{1}{P_\infty}\frac{d^2}{dh^2}[hB(1+h)]-\frac{d}{dh}[hB(1+h)]+2[hB(1+h)] = O(1/K) \quad \text{(A7)}$$

with $1\geqslant h\gg 2/K$, whose solution is

$$B(1+h)=b(2-P_\infty h)+c\left[-\frac{(1-P_\infty h)e^{-P_\infty(1-h)}}{P_\infty(h+2/K)} + (2-P_\infty h)e^{-P_\infty}\int_0^h dh'\frac{e^{P_\infty h'}}{h'+2/K}\right], \quad \text{(A8)}$$

where b and c are constants and $1\geqslant h\gg 2/K$. The corresponding solution for $B(h)$ is then

$$B(h)=b(1-P_\infty h)+c\left[e^{-P_\infty(1-h)} + (1-P_\infty h)e^{-P_\infty}\int_0^h dh'\frac{e^{P_\infty h'}}{h'+2/K}\right]. \quad \text{(A9)}$$

It is important to stress that the above equations give the solution only when $h\geqslant 2/K$. To satisfy Eqs. (A1) and (A3) when $h\sim 2/K$ or smaller, one must include in $B(1+h)$ an additional component that is a $O(1/K)$ when $h\gg 2/K$ and is non negligible only when $h\sim 2/K$. The full solution for $0\leqslant h\leqslant 1$ is then obtained as

$$B(1+h)=b(2-P_\infty h)+c\left[-\frac{(1-P_\infty h)e^{-P_\infty(1-h)}}{P_\infty(h+2/K)} + (2-P_\infty h)e^{-P_\infty}\int_0^h dh'\frac{e^{P_\infty h'}}{h'+2/K}\right]+\frac{d}{K(h+2/K)} + O(1/K). \quad \text{(A10)}$$

It is easy to verify that Eq. (A9) is still the full solution to a $O(1/K)$ for $0\leqslant h\leqslant 1$ and that, from Eq. (A5), the solution for $B(2+h)$, $0\leqslant h\leqslant 1$, is equal to

$$B(2+h)=\frac{1}{(1+h)}\left\{B(2)+bh(4-P_\infty h) - \frac{c}{P_\infty}\left[(3-P_\infty h)e^{-P_\infty(1-h)} + [2-4P_\infty h+(P_\infty h)^2]e^{-P_\infty}\int_0^{h'}\frac{e^{P_\infty h'}}{h'+2/K}\right] + O(1/K)\right\}. \quad \text{(A11)}$$

The constants b, c, d, and $B(2)$ are determined by the various sum rules as well as by the condition, which comes from the structure of the hierarchy of kinetic equations, that $B(h)$ is a piecewise continuous function, namely,

$$B(1)=2b-\frac{c}{2}+\frac{d}{2} = b(1-P_\infty)+c[1+(1-P_\infty)e^{-P_\infty}E_i(P_\infty)]+O(1/K), \quad \text{(A12)}$$

$$B(2)=b(2-P_\infty)+c\left[-\frac{1}{P_\infty}+1(2-P_\infty)e^{-P_\infty}E_i(P_\infty)\right] + O(1/K), \quad \text{(A13)}$$

where $E_i(x)=e^x/x+e^x\int_0^\infty dt\,\exp(-t)/(x-t)^2$.

The result can be expressed as

$$B(0)=b=P_\infty+1 \quad \text{(A14)}$$

$$B(1)=(P_\infty+1)\left[-(P_\infty-1)+2(P_\infty+1)\times\frac{(1-P_\infty\Phi_1^\infty)[1+(1-P_\infty)\Phi_i^\infty]}{1+(1-P_\infty)(\Phi_1^\infty+\Phi_i^\infty)-P_\infty(2-P_\infty)\Phi_1^\infty\Phi_i^\infty}\right] \tag{A15}$$

$$B(2)=(P_\infty+1)\left[2-P_\infty+2\frac{(P_\infty+1)}{P_\infty}\times\frac{(1-P_\infty\Phi_1^\infty)[P_\infty-1+P_\infty(2-P_\infty)\Phi_i^\infty]}{1+(1-P_\infty)(\Phi_1^\infty+\Phi_i^\infty)-P_\infty(2-P_\infty)\Phi_1^\infty\Phi_i^\infty}\right], \tag{A16}$$

where we have introduced the notation $\Phi_i^\infty=e^{-P_\infty}E_i(P_\infty)$ and $\Phi_1^\infty=e^{P_\infty}E_1(P_\infty)$ with $E_1(x)=\int_1^\infty dt e^{-xt}/t$. The values of c and d can be trivially derived from the above equations.

The relaxation rate $\Gamma=\gamma K$ can be obtained by inserting the above solution into Eq. (29), which leads to

$$\Gamma K^2=\gamma K=2P_\infty(1+P_\infty)^2\frac{1-U_\infty}{1+U_\infty} \tag{A17}$$

with

$$U_\infty=\frac{\Phi_1^\infty+\Phi_i^\infty-2P_\infty\Phi_1^\infty\Phi_i^\infty}{(1-P_\infty\Phi_1^\infty)(1-P_\infty\Phi_i^\infty)}. \tag{A18}$$

When $P_\infty\to\infty$, one has

$$\Phi_1^\infty\simeq\frac{1}{P_\infty}\left[1-\frac{1}{P_\infty}+\frac{2}{P_\infty^2}+O\left(\frac{2}{P_\infty^3}\right)\right], \tag{A19}$$

$$\Phi_i^\infty\simeq\frac{1}{P_\infty}\left[1+\frac{1}{P_\infty}+\frac{2}{P_\infty^2}+O\left(\frac{2}{P_\infty^3}\right)\right]. \tag{A20}$$

Inserting Eqs. (A19) and (A20) in Eqs. (A18) and (A17) leads to Eq. (32).

[1] H.M. Jaeger and S.R. Nagel, Rev. Mod. Phys. **68**, 1259 (1996).
[2] J.B. Knight, C.G. Fandrich, C.N. Lau, H.M. Jaeger, and S.R. Nagel, Phys. Rev. E **51**, 3957 (1995).
[3] T. Boutreux and P.G. de Gennes, Physica A **244**, 59 (1997).
[4] S.F. Edwards and D.V. Grinev, Phys. Rev. E **58**, 4758 (1999).
[5] E. Caglioti, V. Loreto, H.J. Herrmann, and M. Nicodemi, Phys. Rev. Lett. **79**, 1578 (1997).
[6] S.J. Linz, Phys. Rev. E **54**, 2925 (1996).
[7] G. Peng and T. Ohta, Phys. Rev. E **57**, 829 (1996).
[8] E.R. Nowak, J.B. Knight, M. Povinelli, H.M. Jaeger, and S.R. Nagel, Powder Technol. **94**, 79 (1997).
[9] E.R. Nowak, J.B. Knight, E. Ben-Naim, H.M. Jaeger, and S.R. Nagel, Phys. Rev. E **57**, 1971 (1998).
[10] X. Jin, G. Tarjus, and J. Talbot, J. Phys. A **27**, L195 (1994).
[11] P.L. Krapivsky and E. Ben-Naim, J. Chem. Phys. **100**, 6778 (1994).
[12] E. Ben-Naim, J.B. Knight, E.R. Nowak, H.M. Jaeger, and S.R. Nagel, Physica D **123**, 380 (1998).
[13] J. Talbot, G. Tarjus, and P. Viot, J. Phys. A **32**, 2997 (1999).
[14] J.W. Evans, Rev. Mod. Phys. **65**, 1281 (1993).
[15] P.R. Van Tassel, J. Talbot, P. Viot, and G. Tarjus, Phys. Rev. E **56**, R1299 (1997).
[16] This assumption is not valid for a process which evolves far from equilibrium, like the RSA model. In this latter case, the factorization property is not satisfied. See, P. Viot, G. Tarjus, and J. Talbot, Phys. Rev. E **48**, 480 (1993).
[17] J.-P. Bouchaud, L.F. Cugliandolo, J. Kurchan, and M. Mezard, in *Spin Glasses and Random Fields*, edited by A.P. Young (World Scientific, Singapore, 1998), p. 161.
[18] M.P. Allen and D.J. Tildesley, *Computer Simulation of Liquids* (Oxford Science Publications, Oxford, 1987).
[19] A.J. Kolan, E.R. Nowak, and A.V. Tkachenko, Phys. Rev. E **59**, 3094 (1999).
[20] C. W. Gardiner, *Handbook of Stochastic Methods* (Springer-Verlag, Berlin, 1990).
[21] B. Bonnier, D. Boyer, and P. Viot, J. Phys. A **27**, 3671 (1994).